ISSN 0020-1685, Inorganic Materials, 2015, Vol. 51, No. 4, pp. 331–339. © Pleiades Publishing, Ltd., 2015.
Original Russian Text © S.R. Egorova, A.A. Lamberov, 2015, published in Neorganicheskie Materialy, 2015, Vol. 51, No. 4, pp. 383–390.

Formation and Distribution of Phases during the Dehydration of Large Hydrargillite Floccules

S. R. Egorova and A. A. Lamberov

Kazan Federal University, Kremlevskaya ul. 18, Kazan, 420008 Tatarstan, Russia
e-mail: segorova@rambler.ru

Received August 7, 2014

Abstract—The phase composition and phase distribution of large floccules of hydrargillite dehydration products obtained by heat treatment at temperatures from 250 to 500°C have been studied by thermal analysis, X-ray diffraction, and IR spectroscopy. Heat treatment in the range 250–300°C leads to the formation of macrocrystalline and microcrystalline boehmite particles. The macrocrystalline boehmite is formed from large hydrargillite crystals. The microcrystalline boehmite results from the "fragmentation" of the hydrargillite crystals. The IR spectra of the samples point to an increase in the number of hydroxyls with $\nu(OH) = 3471\ cm^{-1}$ on the lateral faces of the hydrargillite crystals. The crystallite size of the hydrargillite crystals decreases by a factor of 1.8–2.3. In the floccules, a layer of the macrocrystalline boehmite surrounds a microcrystalline boehmite core. The outer surface is covered predominantly with χ-Al_2O_3. Heat treatment at $t \geq 350$°C leads to γ-Al_2O_3 formation through sequential dehydration of microcrystalline and then macrocrystalline boehmite particles.

DOI: 10.1134/S0020168515030024

INTRODUCTION

The phase transformations of hydrargillite are well studied [1–9]. The paths of the phase transitions of hydrargillite have been determined at both low and high heating rates. Under near-equilibrium conditions [2] in air, the thermal decomposition of large particles proceeds through the formation of boehmite and χ-Al_2O_3. Boehmite forms as a consequence of the hindered diffusion of the released water, resulting in hydrothermal conditions [2]. To ensure χ-Al_2O_3 crystallization, the water should be removed from the reaction zone, which is possible in particles <1 μm in size or after large hydrargillite particles flake off, resulting in the formation of large pores [1, 2, 9]. At high heating rates in the course of thermochemical or thermocentrifugal activation [4, 5], hydrargillite converts to amorphous aluminum oxide.

At present, there is no general consensus as to the rate-limiting step in boehmite formation. According to Brown et al. [10], the rate of the process is limited by water diffusion and desorption, whereas in a number of reports [6–8, 11, 12] the formation and/or growth of boehmite crystal nuclei was thought to be rate controlling. The reported activation energies of the process range from 14 to 313 kJ/mol [7–9, 11–13], which can be accounted for in terms of different treatment and phase composition assessment conditions. Moreover, little is known about phase localization in large floccules of hydrargillite dehydration products [12]. Clearly, precise knowledge of the mechanisms underlying the formation of boehmite and aluminum oxides, the activation energies of the processes, and the phase distribution in the hydrargillite dehydration products in the form of large floccules is currently of special practical importance, because they find wide application as precursors or direct supports of catalysts for petrochemical processes, such as paraffin dehydrogenation and oxidative paraffin chlorination, in which hydrocarbons are brought into contact with a catalyst under fluidization conditions. Hydrargillite floccules range in size from 0.1 to 500 μm, which allows one to synthesize catalysts of tailored granule size from such floccules. Hydrargillite is not used as a catalyst support because of its small specific surface area (<1 m^2/g).

One viable approach to the preparation of supports and catalysts is the dehydration of large hydrargillite floccules at atmospheric pressure. The properties of supports and catalysts can then be tuned and controlled even in the stage of hydrargillite phase transitions. As a consequence, it is of great current interest to study the effect of heat treatment conditions on the phase transformations in large floccules, the phase formation kinetics of boehmite and aluminum oxides, and their distribution in the floccules.

The purpose of this work was to study the formation and distribution of phases during the dehydration of large hydrargillite floccules at atmospheric pressure in air.

Table 1. Effect of the heat treatment conditions of hydrargillite on the crystallite size and composition of the boehmite phase

t, °C	τ, min	Crystallite size, nm						wt %	
		HG		Bm + MBm mixture		calculated for MBm		Bm	MBm
		$D_{(002)}$	$D_{(110)}$	$D_{(020)}$	$D_{(120)}$	$D_{(020)}$	$D_{(120)}$		
–	–	67.5	55.0	–	–	–	–	–	–
250	60	65.8	57.0	50.2	38.6	–	–	100	–
	180	58.5	55.0	51.3	40.4	–	–	100	–
	300	57.6	55.0	50.2	42.3	–	–	100	–
	540	54.8	55.0	48.5	40.6	–	–	100	–
300	180	36.2	30.0	37.8	36.8	11.8	28.9	68.1	31.9
	240	34.0	29.9	36.7	34.9	10.9	23.9	66.4	33.9
	300	–	–	39.7	35.5	17.4	24.7	68.4	31.6
350	60	30.3	27.2	37.6	36.2	7.2	25.8	70.9	29.1
	180	–	–	38.0	33.0	5.1	12.8	73.3	25.7
	300	–	–	40.0	34.7	2.0	12.3	79.4	20.6
400	60	–	–	40.0	34.0	2.4	9.7	78.9	21.1
	180	–	–	41.6	40.4	–	–	100	–
	540	–	–	39.2	40.6	–	–	100	–
450	300	–	–	36.4	40.6	–	–	76.9	–
500	180	–	–	41.6	41.2	–	–	31.0	–

EXPERIMENTAL

The starting material in this study was GD00 hydrargillite, ranging in floccule size from 40 to 180 μm. It was dehydrated in a muffle furnace in the range 250 to 500°C at a rate of 5°C/min in air.

The phase composition of the products was determined by X-ray diffraction on a Shimadzu XRD-7000 diffractometer using long-wavelength CuK_α radiation and a graphite monochromator (angular range 2θ = 5°–90°, scan step of 0.05°). The phases present were identified according to the presence of diffraction peaks of γ-$Al(OH)_3$ (ICSD no. 200 599), γ-AlOOH (ICSD no. 6162), γ-Al_2O_3 (ICSD no. 66 559), and χ-Al_2O_3 (ICSD no. 13-373). The crystallite size was evaluated using the Scherrer formula. The error of crystallite size determination was ≈10%.

Thermal analysis (TA)[1] was carried out with a Netzsch STA-449C Jupiter simultaneous TG–DSC system in combination with an Aeolos QMS 403 quadrupole mass spectrometer in the range 30–1000°C at a heating rate of 10°C/min in flowing argon.

The particle size was determined using a Malvern Mastersizer 2000 laser diffraction analyzer, having a measurement range from 0.1 to 1000 μm.

IR spectra were taken on a Bruker VERTEX 70 FTIR spectrometer at room temperature, using samples pressed with KBr. The spectra were measured with a resolution of 1 cm^{-1} and were averaged over 128 scans. Spectral lines were decomposed into Gaussian components and optimized using ORIGIN software.

Fine particles of hydrargillite dehydration products were obtained via the surface spalling of floccules in the course of attrition in a boiling bed in flowing air for 8 h.

RESULTS AND DISCUSSION

The dehydration products contained two types of boehmite phase (Fig. 1): macrocrystalline (Bm) and microcrystalline (MBm). The oxide phase consisted of χ-Al_2O_3 or a mixture of χ-Al_2O_3 and γ-Al_2O_3. Hydrargillite (HG) converts to Bm at a temperature as low as 250°C (Fig. 1). In contrast to the differential scanning calorimetry (DSC) curve of the parent hydrargillite, those of the samples show an increase in weight loss in the range 450–620°C, due to Bm dehydration to γ-Al_2O_3 (Fig. 2). The average crystallite sizes of Bm are $D_{(020)}$ = 50.5 nm and $D_{(120)}$ = 40.5 nm, which is close to the crystallite size of hydrargillite (Table 1). According to calculations of kinetic parameters [10], the rate-limiting step is the formation and/or growth of platelike nuclei of Bm crystals (Table 2), in agreement with previous results [6, 7, 11]. The kinetic curves for Bm formation can be described

[1] The measurements were performed at the Federal Shared Facilities Center, Kazan Federal University, and were supported by the Federal Agency for Science and Innovations (A.V. Gerasimov).

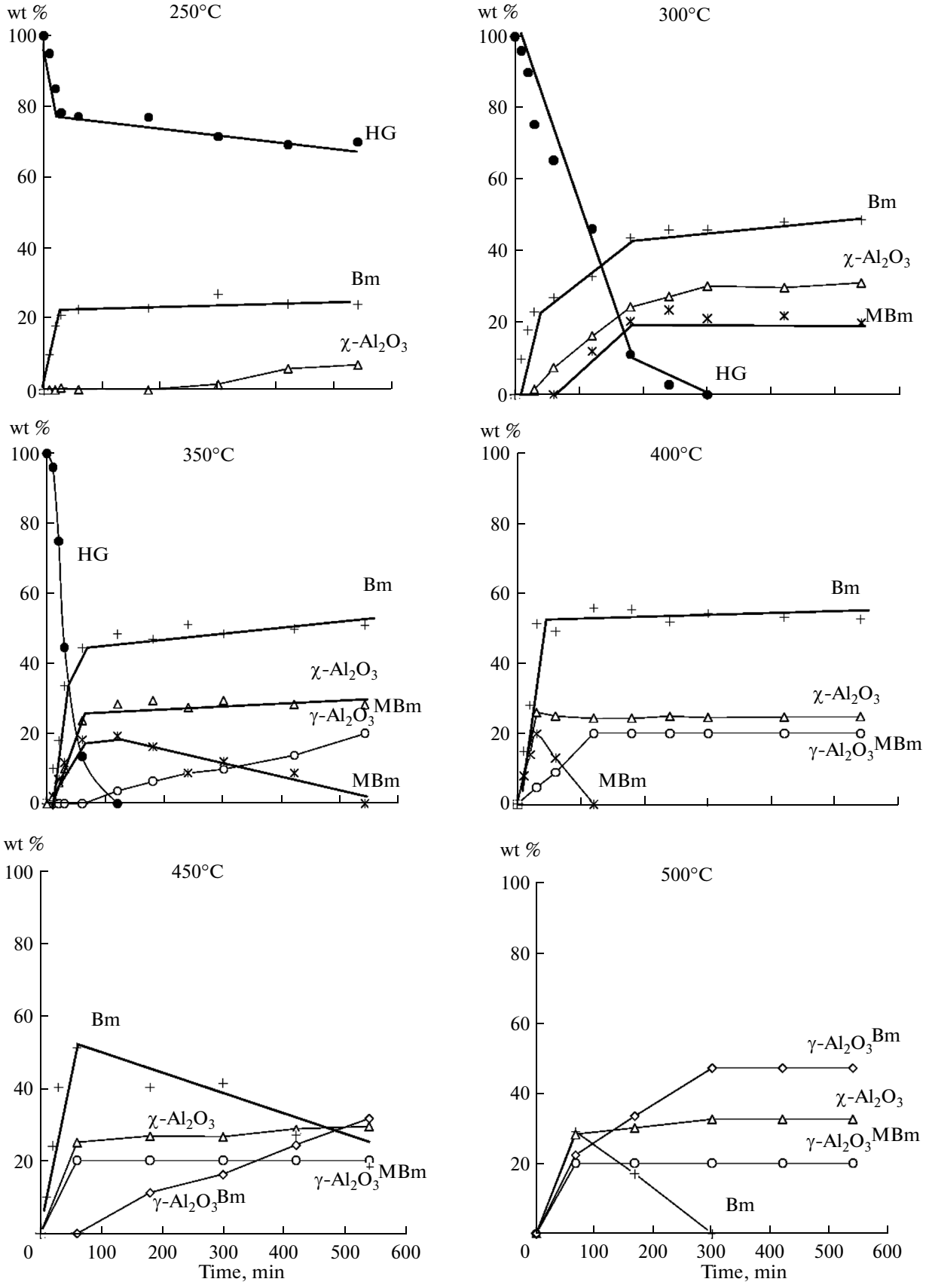

Fig. 1. Kinetic curves for hydrargillite conversion and formation of aluminum hydroxides and oxides.

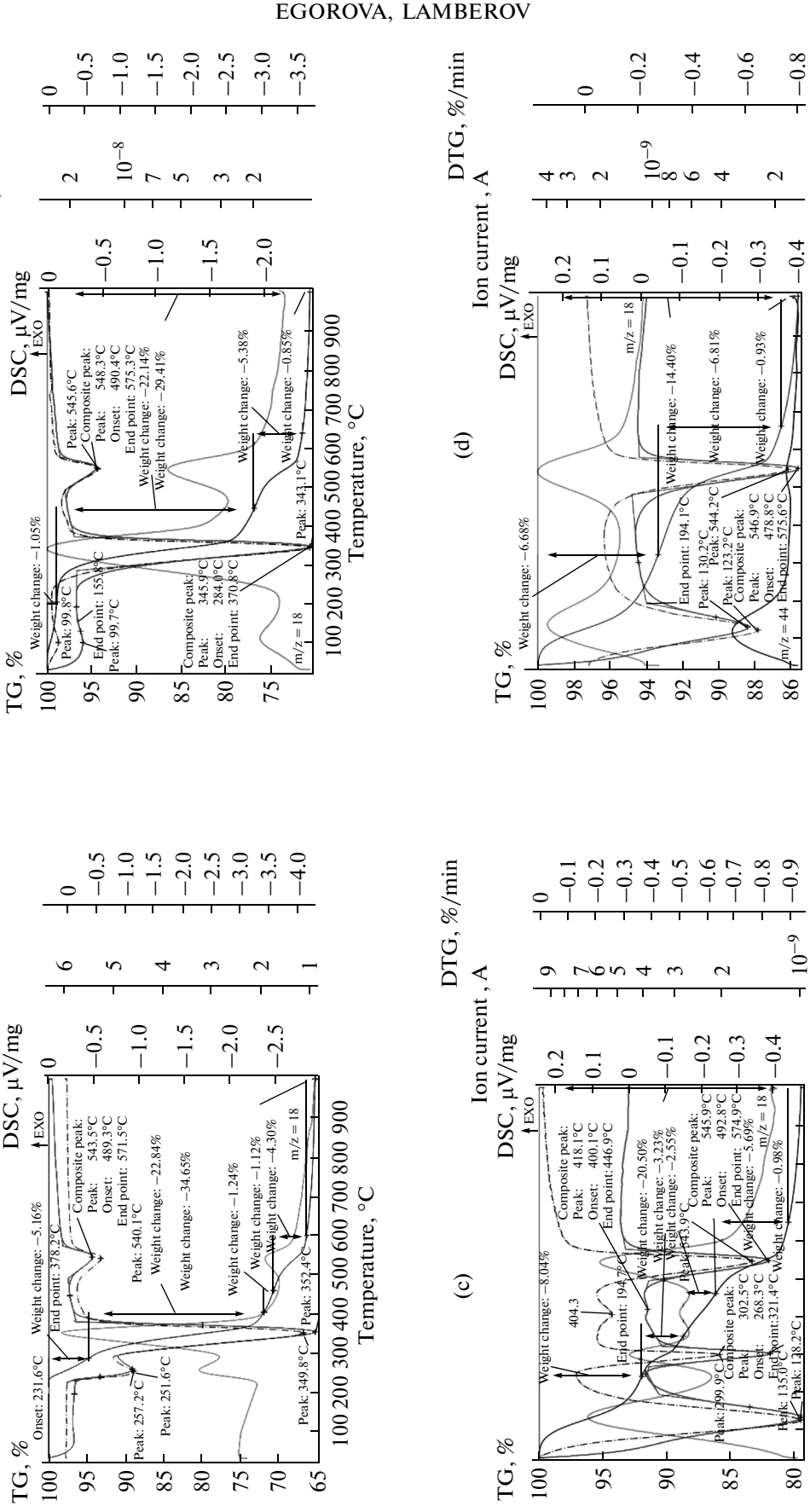

Fig. 2. Thermoanalytical curves of the parent hydrargillite (a) and samples obtained by heat treatment at $t = 250°C$ for $\tau = 420$ min (b), at $t = 300°C$ for $\tau = 300$ min (c), and at $t = 400°C$ for $\tau = 300$ min (d).

Table 2. Kinetic characteristics of various reactions during the thermal decomposition of hydrargillite (Avrami–Erofeev–Kolmogorov function [10])

t, °C	k, s^{-1}	n	R^2	E_a, kJ/mol
HG dehydration				
200	6.2×10^{-6}	1.5	0.8807	74 ± 4
250	2.2×10^{-4}	1.5	0.9903	
300	2.4×10^{-4}	1.5	0.9938	
350	4.1×10^{-4}	2.0	0.9698	
Bm formation				
200	6.2×10^{-6}	1.5	0.8807	62 ± 4
250	1.4×10^{-4}	1.5	0.9695	
300	2.2×10^{-4}	1.5	0.9387	
400	5.8×10^{-4}	2.0	0.9478	
MBm formation				
300	5.0×10^{-5}	1.5	0.9581	94 ± 7
350	1.4×10^{-4}	1.5	0.9961	
400	3.7×10^{-4}	2.0	0.9996	
Al_2O_3 formation				
250	8.5×10^{-6}	2.0	0.9430	86 ± 6
350	7.3×10^{-5}	2.0	0.9175	
400	1.6×10^{-4}	1.5	0.9324	
500	4.8×10^{-4}	2.0	0.9467	

by the Avrami–Erofeev–Kolmogorov equation, and the apparent activation energy (E_a) is 74 ± 4 kJ/mol (Table 2).

Quantitative MBm formation (Fig. 1) is evidenced by the presence of an additional, prominent endothermic peak in DSC curves in the range ≃320–460°C (Fig. 2). Comparison of thermal analysis and X-ray diffraction data leads us to assign this peak to the dehydration of boehmite particles in γ-Al_2O_3. In the X-ray diffraction patterns of the samples (Fig. 3), the reflections from boehmite broaden, but their position (2θ angle) remains unchanged, suggesting that the content of structural water also does not vary (1.02 mol of H_2O per mole of Al_2O_3). The crystallite size evaluated from the contribution of the forming aluminum hydroxide to this quantity is considerably smaller than that of Bm (Table 1), indicating that it has a microcrystalline nature (MBm). Calculations of kinetic parameters (Table 2) suggest a general mechanism for the formation and growth of nuclei of crystals of both boehmites, but E_a for boehmite formation exceeds that for Bm formation (Table 2), which is caused by the preliminary "fragmentation" of the hydrargillite precursor crystals.

Fragmentation is also evidenced by IR spectroscopy data (Fig. 4) for the samples containing both MBm and residual HG. Fragmentation differs from delamination of hydrargillite particles [1]. In the former case, the crystallite size decreases considerably, whereas in the latter it remains almost unchanged. For example, in the IR spectra of the samples prepared at 250°C and containing ≃70 wt % unreacted hydrargillite, with only slight changes in crystallite size (Table 1), delamination causes a considerably larger decrease in the intensity of the absorption band at ν(OH) = 3528 cm^{-1}, arising from stretching vibrations of the interlayer hydrogen-bonded OH groups between the hydrargillite slabs [14], in comparison with the intensity of the absorption band at ν(OH) = 3624 cm^{-1}, due to vibrations of the terminal OH groups in the (001) plane of the crystals [14–16], and with that of the bands at ν(OH) = 3471 cm^{-1} and ν(OH) = 3393 and 3375 cm^{-1}, arising from vibrations

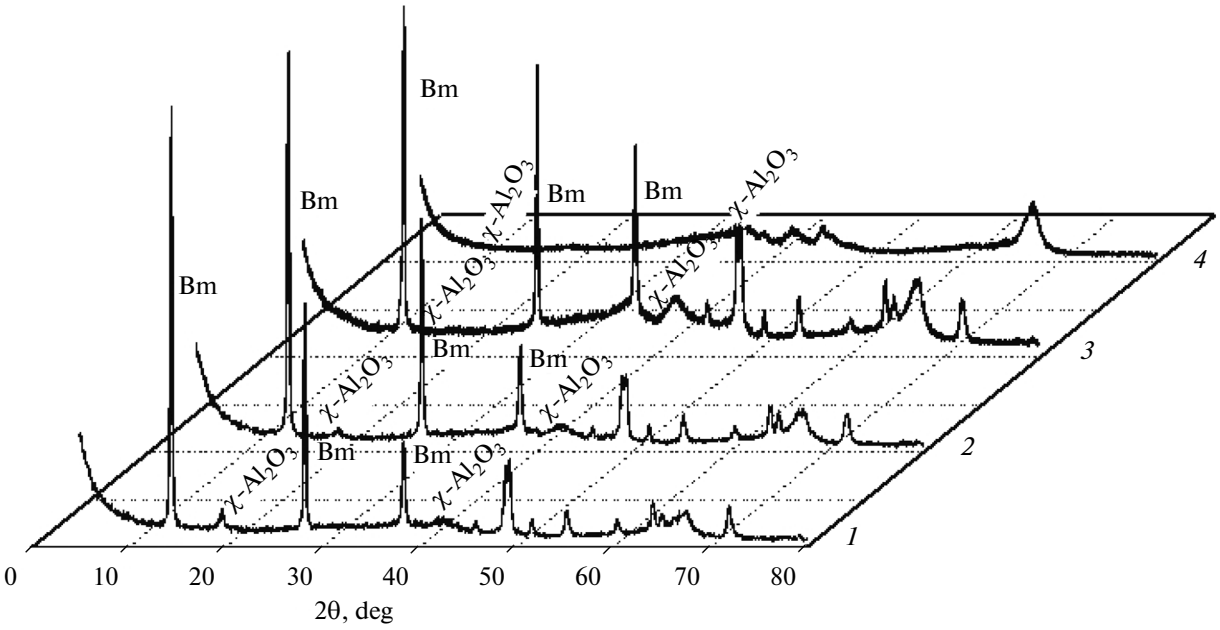

Fig. 3. X-ray diffraction patterns of the hydrargillite dehydration products obtained by heat treatment at (*1*) $t = 300°C$ for $\tau = 300$ min, (*2*) at $t = 400°C$ for $\tau = 300$ min, (*3*) at $t = 450°C$ for $\tau = 300$ min, and (*4*) at $t = 500°C$ for $\tau = 300$ min.

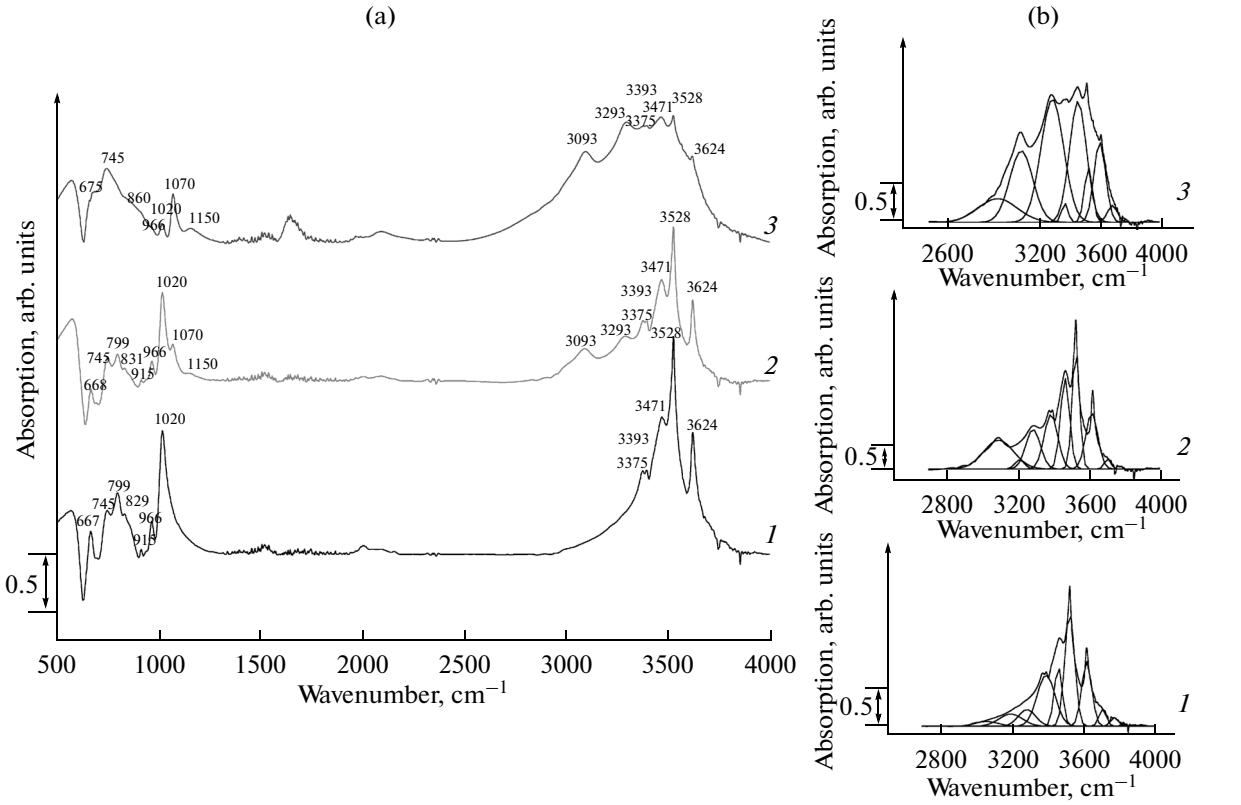

Fig. 4. (a) IR spectra of the parent hydrargillite (*1*) and thermal decomposition products obtained by heat treatment at $t = 250°C$ for $\tau = 300$ min (*2*) and at $t = 350°C$ for $\tau = 60$ min (*3*); (b) portions of the IR spectra after decomposition into Gaussians.

of the OH groups located on the lateral faces of the crystals and in the plane of the hydrargillite slabs, respectively [18]. At 300°C, as the fraction of converted hydrargillite approaches 100 wt % and that of the forming boehmite phase approaches its maximum level (Fig. 1), the reduction in the intensities of the absorption bands at ν(OH) = 3624 and 3528 cm^{-1} is accompanied by an increase in the intensity of the absorption bands at ν(OH) = 3393 and 3375 cm^{-1} and stabilization of the intensity of the band at ν(OH) = 3471 cm^{-1} (Fig. 5). The increase in the former case is due to the influence of the neighboring absorption bands arising from stretching vibrations of the OH groups of boehmite (ν(OH) = 3093 and 3293 cm^{-1}), whose intensity rises by almost a factor of 1.5 (Fig. 4). In the latter case, there is no influence of boundary absorption bands: on the contrary, the intensity of the band at ν(OH) = 3528 cm^{-1} decreases. Analysis of the IR spectra after decomposition into Gaussians demonstrates that the area of the absorption band at ν(OH) = 3471 cm^{-1} increases (Fig. 6), suggesting an increase in the amount of OH groups on the lateral faces of the hydrargillite crystals because of their fragmentation. In addition, the crystallite size of the crystals decreases by a factor of 1.8–2.3 (Table 1), correlating with the area of the absorption band at ν(OH) = 3471 cm^{-1} (Fig. 7). Therefore, the hydrargillite crystal fragmentation products are MBm sources. They are concentrated primarily in the central part of the floccules, because the fine particles that flake off from the outer surface of the samples (Table 3) contain almost a factor of 2 less MBm than do the parent floccules.

In contrast to MBm, the χ-Al_2O_3 phase crystallizes predominantly on the outer surface of the floccules or on the surface of the forming pores [1, 11]. As distinct from the unprocessed floccules (Table 3), the fine particles in all of our samples are enriched in the χ-Al_2O_3 phase, whose content is higher by up to a factor of 4.5

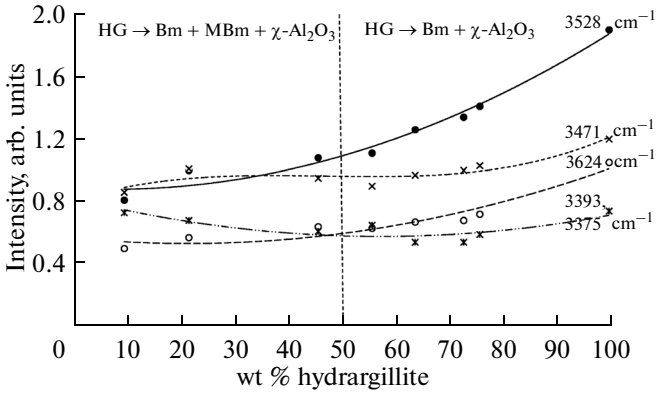

Fig. 5. Effect of hydrargillite concentration on the intensity of absorption bands in the IR spectra of the samples.

in the samples prepared at 250°C and by up to a factor of 1.4–1.6 in those prepared at 300–400°C. The χ-Al_2O_3 content of the dehydration products rises from 8 to 32 wt % in the range 250–300°C and then stabilizes between 350 and 500°C. The crystallite sizes of the crystals are $D_{(440)}$ = 15.0 nm and $D_{(004)}$ = 32.1 nm. The considerable induction period and slow rate of the process attest to a complex physicochemical nature of the formation and growth of platelike nuclei of the χ-Al_2O_3 phase, which requires a long time (≃60–300 min) to reach necessary changes in the structure of the precursor (Table 2, Fig. 1).

With increasing temperature, the percentage of oxide phases in the dehydration products increases on account of $Al_2O_3^{MBm}$ and γ-$Al_2O_3^{Bm}$, resulting from the dehydration of MBm and Bm, respectively (Fig. 1). As in the case of the aluminum compounds considered above, the solid-state reaction is controlled by the formation and growth of platelike nuclei of γ-Al_2O_3 (Table 2). The resulting χ-Al_2O_3 particles are

Table 3. Phase composition of floccules (I) and fine particles (II) obtained by attrition in a boiling bed

Phase	Composition (wt %) of samples produced by heat treatment							
	250°C, 540 min		300°C, 540 min		350°C, 240 min		400°C, 540 min	
	I	II	I	II	I	II	I	II
Hydrargillite	65.0	33.9	–	–	–	–	–	–
Bm	29.0	30.0	48.8	42.5	51.0	45.8	52.9	44.0
MBm	–	–	20.0	9.5	8.7	4.2	–	–
χ-Al_2O_3	8.0	36.1	28.1	44.9	27.5	37.2	24.3	33.2
γ-Al_2O_3	–	–	3.1	3.1	12.8	12.8	22.8	22.8

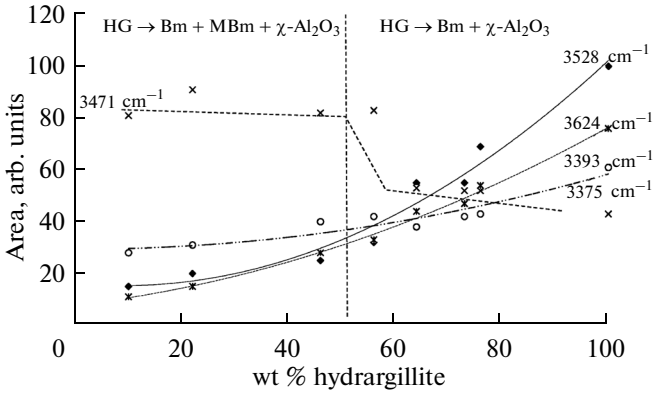

Fig. 6. Effect of hydrargillite concentration on the areas of absorption bands in the IR spectra of the samples after decomposition into Gaussians.

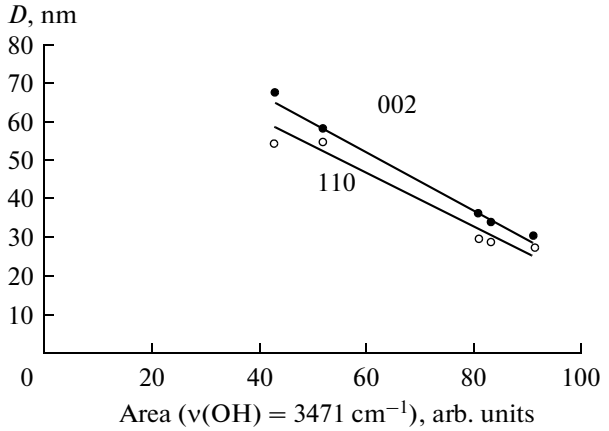

Fig. 7. Correlation between the crystallite size of hydrargillite crystals and the area of the absorption band at ν(OH) = 3471 cm^{-1} in the IR spectra of the samples.

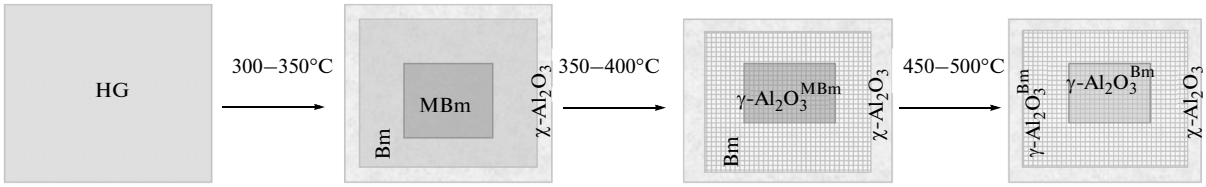

Fig. 8. Schematic of the phase distribution in floccules of hydrargillite decomposing at various dehydration temperatures in air.

much smaller than the γ-Al_2O_3 particles (Table 1). The samples prepared at temperatures from 350 to 400°C have the form of multiphase floccules having an MBm and/or γ-$Al_2O_3^{MBm}$ core, surrounded by a Bm layer and a χ-Al_2O_3 outer (peripheral) layer (Fig. 8). In the samples prepared in the range 450–500°C, the particles comprise a core consisting of γ-$Al_2O_3^{MBm}$ crystals, a Bm and/or γ-$Al_2O_3^{Bm}$ layer, and a χ-Al_2O_3 outer layer (Fig. 8). The outer shape of such multiphase particles remains pseudomorphic with the parent hydrargillite crystals, which in turn allows the floccule shape to persist.

CONCLUSIONS

Heat treatment of hydrargillite floccules in air at temperatures from 250 to 500°C leads to the formation of the phases Bm, MBm, χ-Al_2O_3, γ-$Al_2O_3^{MBm}$, and γ-$Al_2O_3^{Bm}$, consisting of platelike crystals. The solid-state reactions are controlled by the formation and growth of platelike nuclei of the forming phases.

The fragmentation of hydrargillite crystals and the decrease in crystallite size lead to the formation of MBm at 300°C, which crystallizes mainly in the central part of the floccules. The MBm core is surrounded by a Bm layer, which is covered with χ-Al_2O_3, distributed predominantly on the outer surface of the floccules.

The floccules obtained at $t \geq 350$°C have a core consisting of MBm and/or γ-$Al_2O_3^{MBm}$ crystals and surrounded by a layer of platelike crystals of unreacted Bm and/or γ-$Al_2O_3^{Bm}$.

ACKNOWLEDGMENTS

This work was supported by the RF Ministry of Education and Science.

REFERENCES

1. De Boer, J.H., Heuvel, A., and Lonsen, B.G., Studies on pore in catalysis, *J. Catal.*, 1964, vol. 3, no. 3, pp. 268–273.
2. *Physical and Chemical Aspects of Adsorbents and Catalysts*, Linsen, B.G., Ed., London: Academic, 1970.
3. Ivanova, A.S., Aluminum oxide: application, preparation processes, structure, and acid–base properties, *Prom. Katal. Lektsiyakh*, 2009, no. 8, pp. 7–61.
4. Pinakov, V.I., Stoyanovsky, O.I., Tanashev, Yu.Yu., Pikarevsky, A.A., Grinberg, B.E., Dryab, V.N., Kulik, K.V., Danilevich, V.V., Kuznetsov, D.V., and Parmon, V.N., TSEFLAR the centrifugal flash reactor for rapid thermal treatment of powdered materials, *Chem. Eng. J.*, 2005, vol. 107, pp. 157–161.

5. Perander, L.M., Metson, J.B., and Klett, C., Two perspectives on the evolution and future of alumina, in *Light Metals 2011*, Wiley, 2011, pp. 151–155.

6. Lopushan, V.I., Kuznetsov, G.F., Pletnev, R.N., and Kleshchev, D.G., Phase transformations in γ-$Al(OH)_3$ under heat treatment in air and water vapor, *Bull. Russ. Acad. Sci.: Phys.*, 2007, vol. 71, no. 8, pp. 1187–1189.

7. Peric, J., Krstulovic, R., and Vucak, M., Investigation of dehydroxylation of gibbsite into boehmite by DSC analysis, *J. Therm. Anal.*, 1996, vol. 46, pp. 1339–1347.

8. Kleshchev, D.G., Shenkman, A.I., and Pletnev, R.N., *Vliyanie sredy na fazovye i khimicheskie prevrashcheniya v dispersnykh sistemakh* (Effect of Ambient Medium on Chemical and Phase Transformations in Disperse Systems), Sverdlovsk: Ural. Otd. Akad. Nauk SSSR, 1990.

9. Serena, S., Raso, M.A., Rodriguez, M.A., Caballero, A., and Leo, T.J., Thermodynamic evaluation of the Al_2O_3–H_2O binary system at pressure up to 30 MPa, *Ceram. Int.*, 2009, vol. 35, pp. 3081–3090.

10. Brown, M.E., Dollimore, D., and Galwey, A.K., *Reactions in the Solid State*, vol. 22 of *Comprehensive Chemical Kinetics*, Bamford, C.H. and Tipper, C.F.H., Eds., Amsterdam: Elsevier, 1980.

11. Candela, L. and Perlmutter, D.D., Kinetics of boehmite formation by thermal decomposition of gibbsite, *Ind. Eng. Chem. Res.*, 1992, vol. 31, pp. 694–700.

12. Stacey, M.H., Kinetics of decomposition of gibbsite and boehmite and the characterization of the porous products, *Langmuir*, 1987, vol. 3, no. 5, pp. 681–686.

13. Wang, H., Xu, B., Smith, P., Davies, M., DeSilva, L., and Wingate, C., Kinetic modeling of gibbsite dehydration / amorphization in the temperature range 823–923 K, *J. Phys. Chem. Solids*, 2006, vol. 67, pp. 2567–2582.

14. Novak, C., Pokol, G., Izvekov, V., and Novak, T.G., Studies on the reactions of aluminium oxides and hydroxides, *J. Therm. Anal.*, 1990, vol. 36, no. 10, pp. 1895–1909.

15. Phambu, N., Humbert, B., and Burneau, A., Relation between the infrared spectra and the lateral specific surface areas of gibbsite samples, *Langmuir*, 2000, vol. 16, pp. 6200–6207.

16. Kloprogge, J.T., Ruan, H.D., and Frost, R.L., Thermal decomposition of bauxite minerals: infrared emission spectroscopy of gibbsite, boehmite and diaspore, *J. Mater. Sci.*, 2002, vol. 37, pp. 1121–1129.

Translated by O. Tsarev